Characterization of rock thermophysical properties and factors affecting thermal conductivity−A case study of Datong Basin, China

Meng-lei Ji, Shuai-chao Wei, Wei Zhang, Feng Liu, Yu-zhong Liao, Ruo-xi Yuan, Xiao-xue Yan, Long Li

Articles you may be interested in

Research on quality changes and influencing factors of groundwater in the Guanzhong Basin

Journal of Groundwater Science and Engineering. 2017, 5(3): 296-302

Simulation of heat transfer performance using middle-deep coaxial borehole heat exchangers by FEFLOW

Journal of Groundwater Science and Engineering. 2020, 8(4): 315-327   https://doi.org/10.19637/j.cnki.2305-7068.2020.04.002

Discussion on establishing monitoring networks for temperature fields of shallow thermal energy in Shandong, China

Journal of Groundwater Science and Engineering. 2019, 7(1): 86-93   https://doi.org/10.19637/j.cnki.2305-7068.2019.01.009

Electrical-hydraulic conductivity model for a weathered-fractured aquifer system of Olbanita, Lower Baringo Basin, Kenya Rift

Journal of Groundwater Science and Engineering. 2019, 7(4): 360-372   https://doi.org/DOI: 10.19637/j.cnki.2305-7068.2019.04.007

Using TOUGH2 numerical simulation to analyse the geothermal formation in Guide basin, China

Journal of Groundwater Science and Engineering. 2020, 8(4): 328-337   https://doi.org/10.19637/j.cnki.2305-7068.2020.04.003

Scale effects of eroded sediment transport in Wujiang River Basin, Guizhou Province, China

Journal of Groundwater Science and Engineering. 2017, 5(2): 182-192

Original Article

Characterization of rock thermophysical properties and factors affecting thermal conductivity−A case study of Datong Basin, China

Meng-lei Ji[1], Shuai-chao Wei[1,2*], Wei Zhang[1,2], Feng Liu[1,2,3], Yu-zhong Liao[1,2], Ruo-xi Yuan[1,2], Xiao-xue Yan[1,2], Long Li[1]

[1] *Institute of Hydrogeology and Environmental Geology, Chinese Academy of Geological Sciences, Shijiazhuang* 050061, *China.*
[2] *Technology Innovation Center of Geothermal & Hot Dry Rock Exploration and Development, Ministry of Natural Resources, Shijiazhuang* 050061, *China.*
[3] *China University of Geosciences (Beijing), Beijing* 100083, *China.*

Abstract: Rock thermal physical properties play a crucial role in understanding deep thermal conditions, modeling the thermal structure of the lithosphere, and discovering the evolutionary history of sedimentary basins. Recent advancements in geothermal exploration, particularly the identification of high-temperature geothermal resources in Datong Basin, Shanxi, China, have opened new possibilities. This study aims to characterize the thermal properties of rocks and explore factors influencing thermal conductivity in basins hosting high-temperature geothermal resources. A total of 70 groups of rock samples were collected from outcrops in and around Datong Basin, Shanxi Province. Thermal property tests were carried out to analyze the rock properties, and the influencing factors of thermal conductivity were studied through experiments at different temperature and water-filled states. The results indicate that the thermal conductivity of rocks in Datong, Shanxi Province, typically ranges from 0.690 W/(m·K) to 6.460 W/(m·K), the thermal diffusion coefficient ranges from 0.441 mm^2/s to 2.023 mm^2/s, and the specific heat capacity of the rocks ranges from 0.569 KJ/(kg·°C) to 1.117 KJ/(kg·°C). Experimental results reveal the impact of temperature and water saturation on the thermal conductivity of the rock. The thermal conductivity decreases with increasing temperature and rises with high water saturation. A temperature correction formula for the thermal conductivity of different lithologies in the area is proposed through linear fitting. The findings from this study provide essential parameters for the assessment and prediction, development, and utilization of geothermal resources in the region and other basins with typical high-temperature geothermal resource.

Keywords: Datong Basin; Rock thermal conductivity; Thermal diffusivity; Specific heat capacity; Influencing factors

Introduction

The thermophysical parameters of rocks encompass crucial characteristics that define the generation, storage, and transfer of heat within the vari-ous circles of the Earth. These parameters mainly include thermal conductivity, thermal diffusion coefficient and specific heat capacity of rocks (Lei et al. 2018). The thermal physical properties of rocks play a vital role in studying the thermal condition of the deep Earth, the thermal structure of the lithosphere, the distribution characteristics of the geothermal field, and predicting thermal reservoir resource quantities and heat energy extraction rates in geothermal fields (Seipold, 1998; Qiu et al. 2002; Ma et al. 2019; Wang et al. 2023; Liu et al. 2023).

In recent years, many scholars globally have conducted research on the thermophysical properties of rocks, with a primary focus on regional test-

ing and analysis of these properties, as along with factors influencing the thermal conductivity of rocks. Notable regions in China where regional rock thermophysical property tests have been conducted include the Northwest China Basin (Qiu et al. 2002), Erlian Basin (Yu et al. 2020), Songliao Basin (Li et al. 2023), Ordos Basin (Cui et al. 2019), Beijing (Lei et al. 2018), Guizhou (Song et al. 2019; Wei et al. 2022) and others. Studies on factors affecting the thermal conductivity of rocks encompass both internal factors (rock components and structure) and external factors (temperature and pressure) (Zhu et al. 2022). Previous research results indicate that: 1) the thermal conductivity of rocks increases with quartz content (Song et al. 2019; Jesse, 2023) and decreases with porosity (Song et al. 2023), showing a proportional relationship to mineral grain size (Tavman, 1996); 2) rock thermal conductivity decreases with increasing temperature (Hans-Dieter Vosteen, 2003; Wu et al. 2022) and increases with increasing pressure with the latter exerting a smaller effect on thermal conductivity (Seipold and Huenges, 1998); 3) the two factors offset to some extent in high-temperature and high-pressure environments.

In recent years, extensive work related to the exploration and development of geothermal resources has taken place in the Datong Basin, Shanxi Province (Shi, 2019; Zhou, 2021; Pan et al. 2022). Notably, in March 2020, the construction of the DR1 geothermal well in Tianzhen, in the northern part of the Datong Basin, explored high-temperature geothermal fluids at a borehole temperature of 160.2°C (Zhou, 2021). The geothermal wells in the northern part of the Datong Basin were constructed in the same area. With ongoing exploration progress, there is a need to deepen basic research related to geothermal resources within the Datong Basin. This includes conducting rock thermophysical property testing and analysis in the region to gain a more accurate understanding of the thermophysical property distribution of the thermal reservoir lithology. In this paper, rock samples were collected from outcrops in the Datong Basin and its surrounding areas, spanning from the Paleozoic boundary to the Quaternary System. Rock thermal property tests, experiments and analyses were conducted to study the changing law of rock thermal conductivity concerning influencing factors in the area. The results will provide essential parameter bases for the assessment and prediction of geothermal resources in the region and for the development and utilization of the geothermal resources.

1 Regional geothermal geological background

The Datong Basin is situated within the North China Craton, characterized by an eastern belt, an intermediate transition zone, and a western belt. Specifically, the Datong Basin is positioned along the western margin of the middle part of the intermediate transition zone (Zhong et al. 2021), recognized as a Cenozoic faulted basin (Cen et al. 2015). During the Mesozoic, significant lithospheric thinning and craton disruption occurred in the eastern part of the North China Craton produced (Wu et al. 2005; Zhu et al. 2018). The Datong Basin, located at the northern edge of the Central Transform orogenic belt, served as the transition region connecting the Craton disruption and the stabilized Craton. This region experienced significant lithospheric thinning and upwelling of the soft fluvial zone, acting as a heat source and conduit for the formation of regional geothermal resources (Xu et al. 2015; Feng et al. 2022).

While Datong Basin exhibits many missing strata, the surrounding areas have more complete, from old to new, including the Jining Group of the Paleozoic, the Great Wall System and the Jixian System of the Upper Proterozoic, the Cambrian, Ordovician, Carboniferous, and Permian of the Paleozoic, the Jurassic and Cretaceous of the Mesozoic, the Paleocene and Neocene of the Cenozoic, and the Quaternary of the Paleocene and Neoproterozoic (Liu et al. 2021). The Paleozoic Jining Group, consisting of mafic rocks and gneisses, forms the basement of the Basin, and is primarily exposed in the eastern edge and northern part of the basin. Notably, this formation constitutes the lithology of the Tianzhen-Yanggao high-temperature geothermal resource thermal reservoir (Zhou, 2021). The Upper and Middle Paleozoic mainly comprises dolomites, presented in Guangling and Yangyuan. The Paleozoic Cambrian and Ordovician consist of carbonate rocks, distributed in Hunyuan and Lingqiu. The Carboniferous and Permian strata are mainly composed of clastic rocks, mudstone and carbonate rocks, distributed west of the line of goose feather mouth - Louzigou in Huairen County. The Mesozoic Jurassic strata are predominantly clastic rocks and volcanic sedimentary rocks, while the Cretaceous strata are clastic rocks. Neoproterozoic strata are developed with Hannauba basalt, clay and gravel layers, mainly distributed in Fengzhen and Yangyuan Counties. The quaternary strata mainly comprise loose accumulations, including the Pleistocene Shuntian

basalt, a significant stratum in China, and the Pleistocene Zhutian Basalt (Shi, 2019; Liu et al. 2021).

The Datong Basin geothermal system operates as a high-temperature convection-conduction geothermal system (Zhou, 2021). The thermal reservoirs within the geothermal field primarily consist of Paleozoic metamorphic rocks, Tertiary sandstones, and Ordovician greywacke thermal reservoirs (Han et al. 2018). This classification places the geothermal filed under the category of a medium and shallow buried type, economically suitable for exploitation (Wang, 2014), Covering a total area of 5,028.061 km², the basin boasts relatively abundant geothermal resources. The geothermal resources in the area are categorized based on thermal storage characteristics into fissure-type banded thermal storage and pore-type layered thermal storage (Pan et al. 2022).

Within this classification, the Neoproterozoic system exhibits four sets of sandstone thermal reservoirs in the upper, middle, and lower sections of the South Yulin Formation and the Kouzhai Formation, distributed across the region, except for the Sanggan River West Bulge (Pan et al. 2022). Available data indicate that the gneiss thermal reservoirs of the Taikooji gneisses are predominantly found in the Tianzhen−Yanggao fissure zone geothermal field and the Maojiaosapon fracture bulge geothermal field (Zhang et al. 2016). Ordovician−Cambrian tuff thermal reserves are concentrated in Shuo County break-convex geothermal field. Quaternary thermal reservoirs, mainly located in Tianzhen Mawenqi−Shui Bucket Temple Village and the area of Pingshan Village in Yanggao County, consist of shallow thermal reservoirs composed of Quaternary loose sediments (Pan et al. 2022) (Fig. 2).

2 Sample collection and testing

In this study, a total of 70 sets of rock samples were collected, covering a diverse range of strata from the Archean, Proterozoic, Paleozoic, Mesozoic and Cenozoic eras. The collected lithologies predominantly included gneiss, granulite, meta-granulite, diabase, metamonzonitic granite, granite, basalt, marble, sandstone, limestone, dolomite, shale, mudstone, marl, etc. The sampling locations encompassed Tianzhen County, Yanggao County, Yunzhou District, Yungang District, Guangling District, Huairen City, Hunyuan County and Ying County, and other areas (Fig. 1).

Rock thermophysical property tests were conducted using a Hot Disk thermal constant analyzer (Model: TPS1500, Fig. 3), employing the transient planar heat source method. The instrument featured a thermal conductivity test range of 0.005−500 W/(m·K), ensuring a broad test range and high accuracy. Notably, the test required only a flat sample surface without special sample preparation. The analyzer can simultaneously measure three parameters: Thermal conductivity, thermal diffusion coefficient and specific heat capacity.
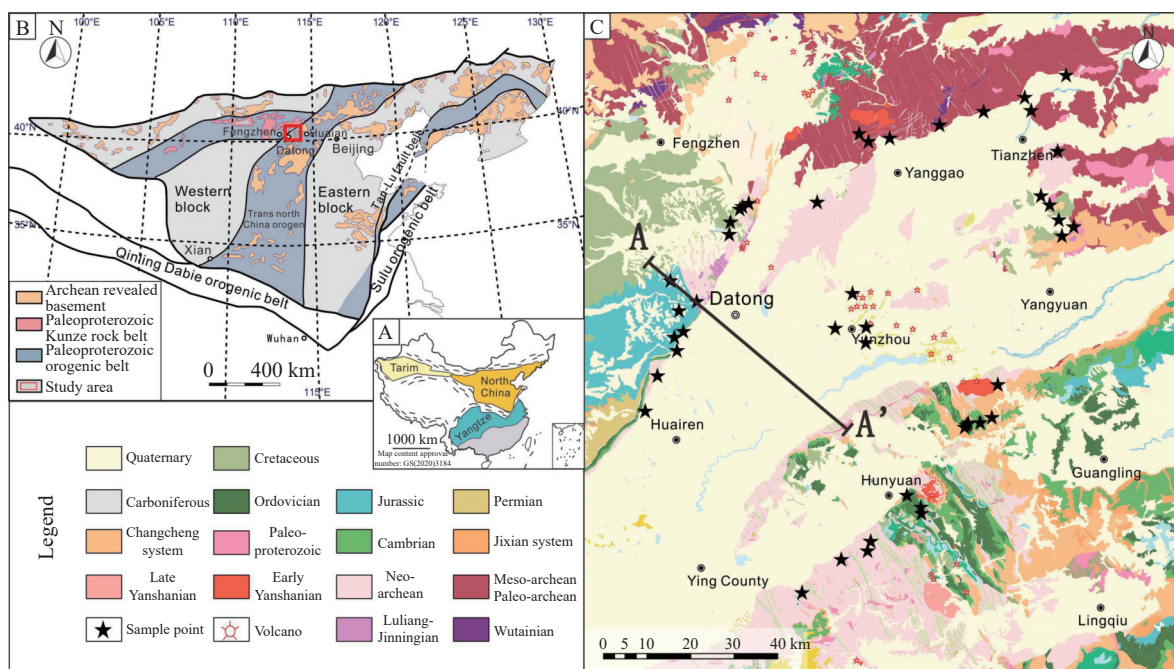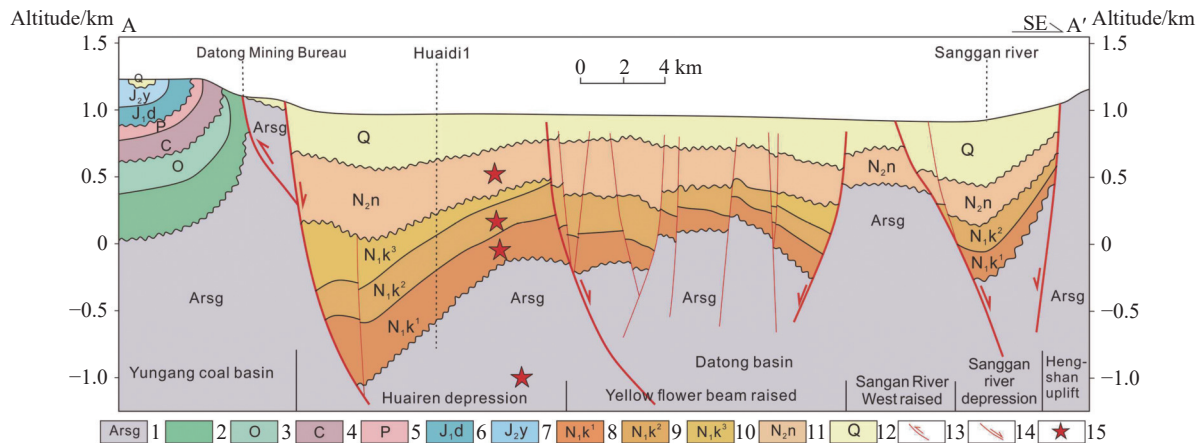

Fig. 1 Location of the study area and distribution of sampling points

Fig. 2 NW-SE geologic structure profile of Datong Basin (The profile position is shown in Fig. 1C, quated from Pan et al. 2022)

Notes: 1-Archaic Sanggan Group; 2-Cambrian; 3-Ordovician; 4-Carboniferous series; 5-Permian system; 6-Lower Jurassic cohorts; 7-Yungang Group of Middle Jurassic; 8-Neogene lower member of Kezhai Formation; 9-Neogene middle section of Kezhai Formation; 10-Neogene Kezhai Formation upper member; 11-Neogene Nanyulin Formation; 12-Quaternary system; 13-Reverse fault; 14-Normal fault; 15-Thermal reservoir
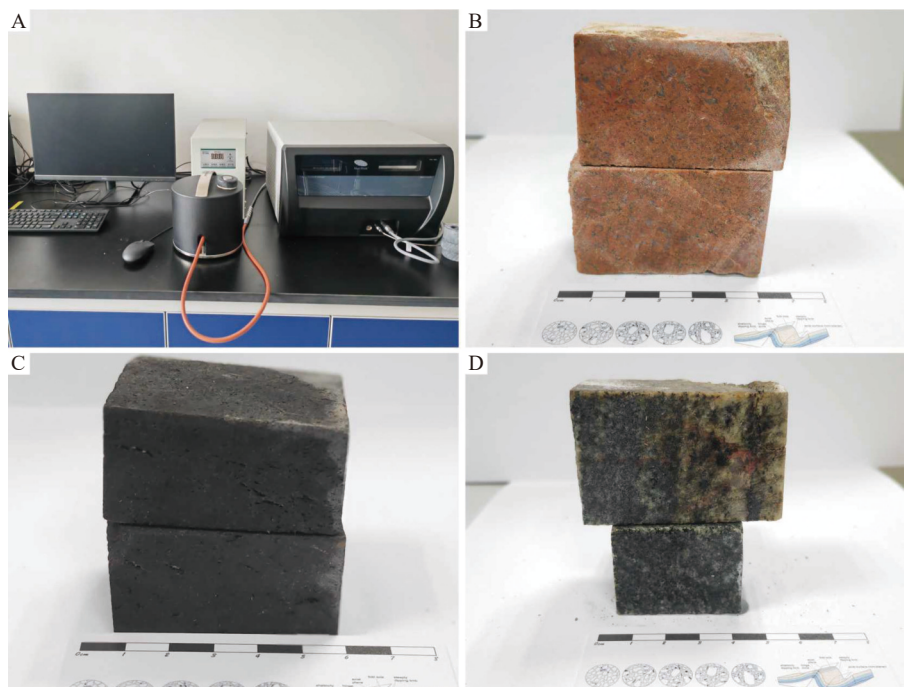
Fig. 3 Hot Disk TPS1500 thermal constant analyzer and processed sample

The experimental design encompassed investigations into the thermal properties of rock at room temperature and pressure, at high temperature, and under water-saturated conditions. High-temperature experiments utilized the Hot Disk TPS1500 tester combined with a heating module, measuring temperatures at 30°C, 60°C, 90°C, 120°C, 150°C and 180°C. For water-saturated experiments, rock samples were initially immersed in distilled water for over 48 hours to allow complete water penetration into the effective pore space of the rock, simulating an underground water-saturated state. Subsequently, thermophysical property tests were conducted on the water-saturated samples.

The density test of rocks adhered to the standards outlined in GB/T 23561.3—2009, titled "Method for Determining Physical and Mechanical Properties of Coal and Rocks Part 3: Method for Determining the Density of Coal and Rock Blocks". The sealing method was employed for the test, utilizing an electronic balance (Model: CPA124S/25292454).

3 Test results of rock thermal properties

3.1 Thermal conductivity

The test results of thermal conductivity of rocks (Fig. 4) show that the thermal conductivity of rocks in the basin predominantly falls within the range of 0.690–6.460 W/(m·K). Categorically, the thermal conductivity of igneous rocks spans 0.690–3.123 W/(m·K), with a mean value of 1.489±0.647 W/(m·K). Metamorphic rock exhibit a range of 1.818–4.346 W/(m·K), with a mean value of 2.567±0.509 W/(m·K). Sedimentary rocks show the broadest range, ranging from 1.308 W/(m·K) to 6.460 W/(m·K), with an average value of 3.510±1.175 W/(m·K). The thermal conductivity among the three major rock types displays evident differences, with igneous rock having the lowest value, followed by metamorphic rock with a more concentrated distribution, and sedimentary rock exhibiting a wide range of variations and higher overall values.

Further classification of rock samples into 12 types based on lithology reveals the average thermal conductivity for each lithology, listed from smallest to largest: Tuff 0.990 W/(m·K), basalt 1.294 W/(m·K), granulite 2.290 W/(m·K), metagranulite 2.300 W/(m·K), granite 2.313 W/(m·K), schist 2.425 W/(m·K), gneiss 2.632 W/(m K) and limestone 2.968 W/(m·K), metamorphic granite 3.030 W/(m·K) and clay rock 3.132 W/(m·K), sandstone 3.460 W/(m·K), dolomite 5.450 W/(m·K).

By comparing the thermal conductivities of the same lithologies in other regions of the North China Craton, including the Jizhong Depression in the eastern land mass (Su, 2021; Gao, 2023), the Ordos Basin in the western land mass (Sun et al. 1996), and the Qingshui Basin in the middle zone,
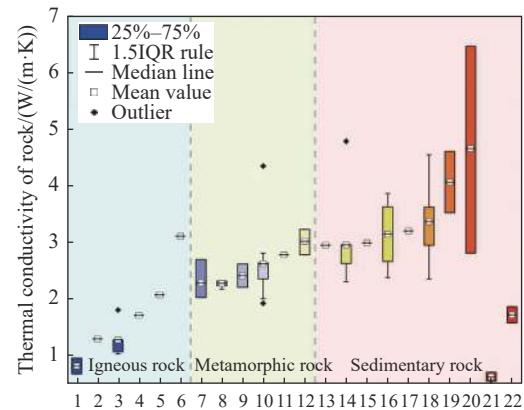
Fig. 4 Thermal conductivity box patterns of different lithologies in Datong Basin

Notes: The serial number of horizontal coordinate is expressed respectively: 1-tuff; 2-tuffaceous breccia; 3-basalt; 4-diabase; 5-monzonitic granite; 6-granite; 7-metagranulite; 8-granulite; 9-schist; 10-gneiss; 11-marble; 12-metamorphic granite; 13-mudstone; 14-limestone; 15-siltstone; 16-shale; 17-marl; 18-sandstone; 19-pebbly sandstone; 20-dolomite; 21-Soil (dry); 22-Soil (saturated)

(Sun et al. 2006; Qi, 2021), indicate distinct patterns (Table 1). Mudstones and sandstones in Datong Basin closely align with those in the Ordos Basin and surpass those in Qinshui Basin and Jizhong Depression. Dolomites and gneisses in Datong Basin exhibit significantly higher thermal conductivity than those in the eastern and western land masses of the North China Craton, while being the lowest in the Ordos Basin. Thermal conductivity values of fine sandstone and granites are slightly higher than those in the Qinshui Basin. Tuff thermal conductivity values are the lowest in Datong Basin, the highest in Ordos Basin, and similar in Qinshui Basin and Jizhong Depression. Overall, the higher thermal conductivity values of rocks in the Datong Basin compared to other areas of the North China Craton may be attributed to the retention and dehydration of the subducting Pacific plate in the mantle transition zone and the up-

Table 1 Comparison between thermal conductivity of different lithologies and other areas of North China Craton

Lithology	Datong basin W/(m·K) (This text)	Ordos Basin W/(m·K) (Sun et al. 1996)	Qingshui Basin W/(m·K) (Sun et al. 2006; Qi, 2021)	Jizhong Depression W/(m·K) (Su, 2021; Gao, 2023)
Mudstone	2.961（1）	1.984±1.032（20）	1.820±0.820（18）	2.350（15）
Sandstone	3.375±0.593（9）	2.943±1.008（46）	2.440±0.280（16）	2.150
Limestone	2.968±0.676（9）	3.668±1.110（10）	3.350±0.490（8）	3.920（9）
Dolomite	5.451±1.486（4）	3.345±1.120（7）	—	5.670（10）
Gneiss	2.632±0.663（9）	1.786（1）	—	2.590（11）
Fine sandstone	2.997（1）	—	2.260±0.740（18）	—
Granite	3.120（1）	—	2.715	—

Notes: Number of samples is shown in brackets

welling of thermal material due to localized mantle convection during the destruction of the North China Craton (Yu, 2021).

3.2 Thermal diffusivity

The thermal diffusivities of majority of rocks in the Datong Basin range from 0.441–2.023 mm²/s, with a mean value of 1.170 mm²/s. Examining the box plots depicting thermal diffusivities across different lithologies (Fig. 5) reveals that the thermal diffusivity of igneous rocks spans 0.441–1.486 mm²/s, with a mean value of 0.700±0.285 mm²/s. Metamorphic rocks exhibit a range of 0.795–1.865 mm²/s, with a mean value of 1.123±0.097 mm²/s. while sedimentary rocks show a range of 0.983–2.023 mm²/s, with a mean value of 1.373±0.243 mm²/s. The trend of thermal diffusivity among the three major lithologies aligns closely with that of thermal conductivity, with igneous rocks having the smallest values, followed by metamorphic rocks and sedimentary rocks. However, the distribution of thermal diffusivity in sedimentary rocks is slightly more concentrated than that of thermal conductivity.
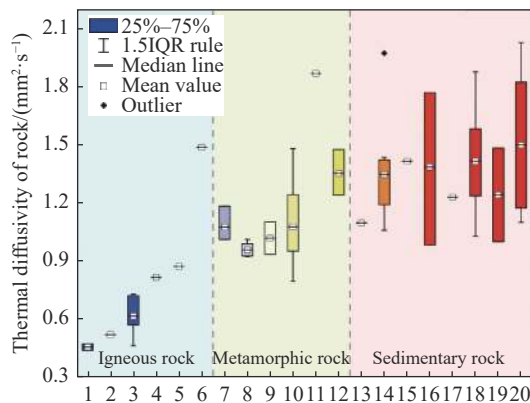

Fig. 5 Box diagram of rock thermal diffusivity in Datong Basin

Notes: The serial number of horizontal coordinate is expressed respectively: 1-tuff; 2-tuffaceous breccia; 3-basalt; 4-diabase; 5-monzonitic granite; 6-granite; 7-granulite; 8-metagranulite; 9-schist; 10-gneiss; 11-marble; 12-metamorphic granite; 13-mudstone; 14-limestone; 15-fine sandstone; 16-shale; 17-marl; 18-sandstone; 19-pebbly sandstone; 20-dolomite

Linear fitting of thermal conductivity and thermal diffusivity for rocks in the study area indicates a clear positive correlation between the two (Fig. 6), expressed by the correlation equation K = 2.733κ−0.415 (R^2 = 0.731, P < 0.0001). Arranging the average thermal diffusivity in descending order for various lithologies yields the following sequence: Tuff 0.479 mm²/s, basalt 0.618 mm²/s, granulite 0.958 mm²/s, schist 1.018 mm²/s, granite 1.059 mm²/s, metagranulite 1.076 mm²/s, gneiss

1.077 mm²/s, claystone 1.295 mm²/s, limestone 1.345 mm²/s, metamorphic granite 1.352 mm²/s, sandstone 1.385 mm²/s, dolomite 1.497 mm²/s.
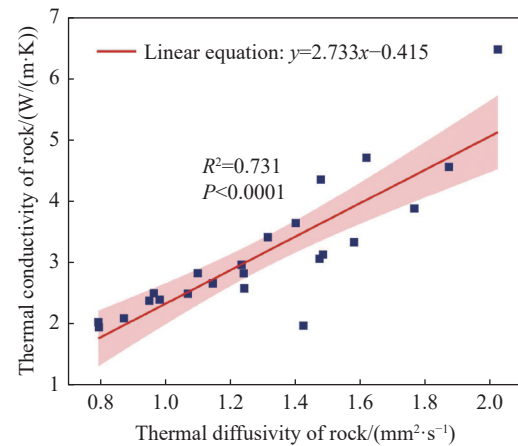

Fig. 6 Relationship between thermal conductivity and thermal diffusivity of rock

3.3 Specific heat capacity

The specific heat capacity of rocks in Datong Basin ranges from 0.569 KJ/(kg·°C) to 1.117 KJ/(kg·°C), with an average value of 0.933 KJ/(kg·°C).

Analyzing the specific heat capacity box diagram for various lithologies (Fig. 7), reveals that igneous rocks have a range of 0.723–1.068 KJ/(kg·°C), with a mean value of 0.830±0.101 KJ/(kg·°C). Metamorphic rocks exhibit a range of 0.742–1.063 KJ/(kg·°C), with a mean value of 0.866±0.098 KJ/(kg·°C), while sedimentary rocks displays a range of 0.688 KJ/(kg·°C) to 1.117 KJ/(kg·°C), with a mean value of 0.901±0.122
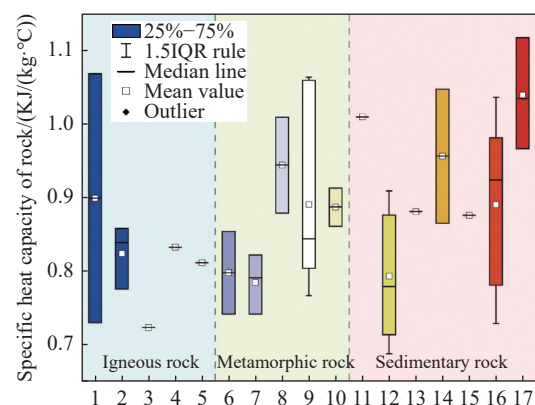
Fig. 7 Box diagram of specific heat capacity of rocks in Datong Basin

Notes: The X axis represents: 1-tuff; 2-basalt; 3-diabase; 4-monzonitic granite; 5-granite; 6-granulite; 7-metagranulite; 8-schist; 9-gneiss; 10-metamorphic granite; 11-mudstone; 12-limestone; 13-fine sandstone; 14-shale; 15-marl; 16-sandstone; 17-dolomite

KJ/(kg·°C). The average difference in specific heat capacity among the three lithologies is not more than 0.500, suggesting that lithology has no pronounced effect on the specific heat capacity of the rocks. In other words, rocks with different lithologies exhibit similar heat storage capacities (Xiong et al. 2020).

Arranging the average specific heat capacity in descending order for various lithologies yields the following sequence: Granulite 0.785 KJ/(kg·°C), granite 0.789 KJ/(kg·°C), metagranulite 0.798 KJ/(kg·°C), basalt 0.824 KJ/(kg·°C), sandstone 0.885 KJ/(kg·°C), metamorphic granite 0.887 KJ/(kg·°C), gneiss 0.891 KJ/(kg·°C), tuff 0.899 KJ/(kg·°C), schist 0.944 KJ/(kg·°C), clay rock 0.947 KJ/(kg·°C), dolomite 1.039 KJ/(kg·°C), limestone 1.286 KJ/(kg·°C).

4 Discussion

The thermal conductivity of rocks is affected by various factors, encompassing both internal and external elements. Internal factors include mineral content, presence of glass, and pore fluids, as well as rock structure involving pore and fissure conditions, mineral distribution, and arrangement. External factors comprise temperature and pressure. Investigating the internal causes aids in establishing predictive models for thermal conductivity, while studying external causes aims to understand how rocks change with temperature and pressure. The derivation of correction formulas is crucial for maximizing the restoration of rock thermal conductivity values in in-situ conditions. This paper focuses on temperature as the primary external factor influencing rock thermal conductivity, conducting experimental research to analyze the relationships between rock thermal conductivity, density, water saturation and lithostratigraphy.

4.1 Temperature

The experimental tests on thermal conductivity of

rocks at various temperatures, i.e. 30°C, 60°C, 90°C, 120°C, 150°C, 180°C, were conducted on samples of different lithologies in the study area. The results, presented in Table 2 and graphically depicted in Fig. 8, reveal a decreasing trend in thermal conductivity for different lithologies as temperature increases. The reduction percentages with increasing temperature are as follows: 36% for dolomite, 26% for shale, 17% for limestone, 16% for metamonzonite granite, 6% for monzonitic granite, and about 6% for gneiss. Notably, carbonate rocks exhibit higher degrees of decrease in thermal conductivity at high temperatures, and the greater the thermal conductivity of rocks at room temperature, the greater the decrease with increasing temperature.
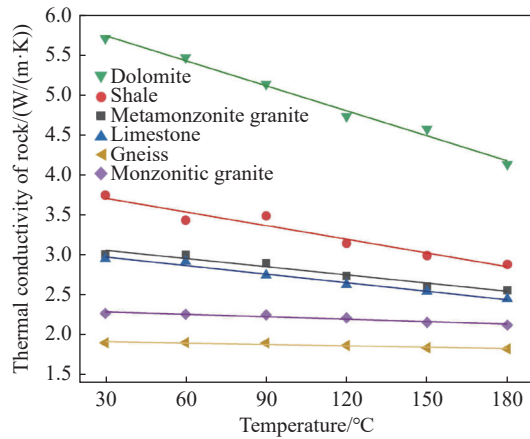
By linear fitting of thermal conductivity and temperature measured at high temperature, a temperature correction formula for the corresponding lithologic thermal conductivity in the Datong Basin is obtained (Table 3). The temperature measurement curves (Fig. 9) from the DR1 well within the Datong Basin (Zhang, 2019) suggested that the average geothermal temperature gradient is 29.3°C/km in the Archaean gneiss thermal reservoir from 1,400 m to 1,605 m (linear warming section), and the temperature at 1,500 m is about 65°C. The temperature-corrected equation thermal conductivity of the gneiss thermal reservoir suggests an in-situ thermal conductivity of 1.907 W/(m·K).

The temperature dependence of thermal conductivity of rock components is illustrated, such as the decrease in the thermal conductivity of CaO with increasing temperature (Fig. 10) (Meng et al. 2022). The transfer of thermal energy in rocks primarily occurs through the vibration of the lattice inside minerals. The thermal conductivity of crystals is influenced by specific heat capacity, phonon velocity, and mean free range of phonons. At high temperatures, it is mainly determined by velocity and the free range (Tan et al. 2004). The vibrational amplitude of the lattice increases with

Table 2 Data of rock thermal conductivity at different temperatures

| Sample Number | Temperature/°C | | | | | | | |
	Lithology	25°C	30°C	60°C	90°C	120°C	150°C	180°C	Reduction/%
GLX-10	Dolomite	6.460	5.701	5.460	5.131	4.727	4.569	4.128	36
GLX-2	Shale	3.873	3.742	3.430	3.484	3.140	2.984	2.876	26
GLX-8	Limestone	2.947	2.947	2.911	2.741	2.624	2.539	2.446	17
TZX-5	Metamonzonite granite	3.055	3.001	2.996	2.892	2.733	2.603	2.554	16
DTA-6	Monzonitic granite	2.264	2.264	2.254	2.246	2.209	2.153	2.119	6
DTB-1	Gneiss	1.939	1.896	1.900	1.894	1.864	1.836	1.821	6

Fig. 8 Relation between thermal conductivity and temperature of rocks

temperature, resulting in larger anharmonic oscillations, more phonon numbers, and more collisions, reduced mean free range of thermal waves, and ultimately a decrease in the thermal conductivity of the rock (Zhao et al. 1995; Miao et al. 2013; Gao, 2015). Additionally, elevated temperatures create a "thermal impedance" between mineral particles, further contributing to the reduction of effective thermal conductivity (Yu et al. 2020).

4.2 Density

The plot of density versus thermal conductivity (Fig. 11) reveals a positive correlation between the thermal conductivity values of igneous and sedimentary rocks and their density among the three major rock types. However, there is no evident correlation between the thermal conductivity of metamorphic rocks and their density. As rocks are porous medium, their density is primarily influenced by factors such as mineral composition, content, porosity, pore fluid composition, and the pressure applied to the rock. Among them, mineral composition, content, and pore distribution are categorized as rock composition factors, while pressure is an environmental factor. Since these

factors impact both thermal conductivity and density, the positive correlation observed between rock density and thermal conductivity suggests a shared underlying influence (Zhu et al. 2022).

Mineral density is determined by a combination of atomic masses, ratios, and bonding modes. The arrangement of atoms and their bonding modes also influences the efficiency of phonon heat transfer, which is reflected on a macroscopic level in the magnitude of thermal conductivity. However, some rocks with similar densities exhibit significantly different thermal conductivities. This discrepancy may arise from similarity in atomic compositions and sizes but differences in chemical bonding, resulting in variations in heat transfer efficiency. Consequently, rocks within the same mineral family with similar crystal structures demonstrate a consistent trend: Higher density corresponds to higher thermal conductivity (Zhu et al. 2022).

4.3 Water saturation

Fig. 12 illustrates that the thermal conductivity of rocks in the water-saturated state exhibits varying degrees of increase compared to the dry state. Clastic rocks, in particular, show a significant difference between the water-saturated state and dry states, with conglomerate-bearing sandstones experiencing the most substantial increase, reaching up to 0.986 W/(m·K), an approximate 35% rise. In contrast, metamorphic rocks and Ordovician tuffs exhibit smaller differences, such as schist, which shows a minimal increase of only 0.016 W/(m·K), equivalent to a 0.7% rise.

This observed variation can be attributed to the fact that the thermal conductivity of water , about 0.600 W/(m·K), is much higher than that of air (0.026 W/(m·K)). Additionally, water, being an infiltrating fluid, adheres to contact points between rock particles and pores, enhancing the thermal conductivity effect and forming a "liquid bridge" for heat flow (Li et al. 2009). The extent of the

Table 3 Temperature correction formula of rock thermal conductivity in Datong Basin

Sample Number	Lithology	Correction formula	R^2
GLX-10	Dolomite	$\lambda(T) = -0.0163(T-T_0)+\lambda(T_0)$	0.895
GLX-2	Shale	$\lambda(T) = -0.0069(T-T_0)+\lambda(T_0)$	0.918
GLX-8	Limestone	$\lambda(T) = -0.0034(T-T_0)+\lambda(T_0)$	0.981
TZX-5	Metamonzonite granite	$\lambda(T) = -0.0033(T-T_0)+\lambda(T_0)$	0.965
DTA-6	Monzonitic granite	$\lambda(T) = -0.0008(T-T_0)+\lambda(T_0)$	0.918
DTB-1	Gneiss	$\lambda(T) = -0.0008(T-T_0)+\lambda(T_0)$	0.979

Note: $\lambda(T_0)$ refers to the thermal conductivity value at room temperature and pressure.
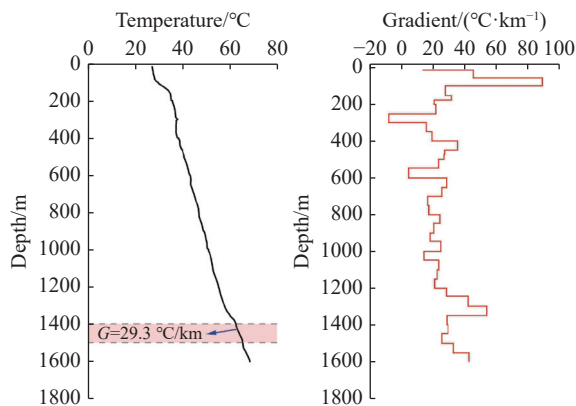
Fig. 9 Temperature measurement curve and ground temperature gradient ladder diagram of well DR1
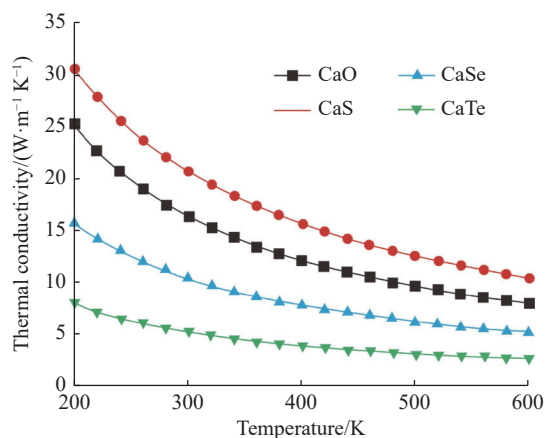
Fig. 10 Relationship between thermal conductivity and temperature of CaM (Meng et al. 2022)

increase in thermal conductivity depends on the porosity of the rock, where rocks with higher porosity absorbs more water after saturation, leading to a greater increment in thermal conductivity. In contrast, low-porosity rocks exhibit minimal changes in thermal conductivity after water saturation (Yang et al. 1986). Therefore, water saturation primarily influences thermal conductivity by creating a "liquid bridge" for heat flow in the rock's porosity, and the difference in thermal conductivity between the water-saturated and dry states indirectly reflects the magnitude of rock's porosity.

4.4 Stratigraphic

By combining the stratigraphy and lithology of rocks in the study area and comparing the thermal conductivity of rocks with the same lithology, a trend emerges where the thermal conductivity generally increase with older age of the strata. For example, the thermal conductivities of Quaternary Cetian basalt and Hannoba basalt are 1.014 W/(m·K), 2.166 W/(m·K), respectively. Similarly, the thermal conductivities of sandstones in the Cretaceous, Jurassic, and Permian formations are 2.225 W/(m·K), 3.220 W/(m·K), and 4.044 W/(m·K), respectively. The thermal conductivity of Ordovician dolomite is 4.702 W/(m·K), while Middle-Proterozoic dolomite is 6.460 W/(m·K). Previous studies have suggested that the older the age of the formation, the longer the compaction time experienced, resulting in a higher compaction degree, denser particle arrangement, and increased thermal conductivity (Song et al. 2019).

However, it is worth noting that some rock samples, like gneiss and saprolite, exhibit no clear pattern between thermal conductivity values and strata. Since the strata represent specific geological eras, either new or old, with an emphasis on the time factor, analyzing the relationship between strata and thermal conductivity becomes challenging due to the difficulty of controlling a single variable in this context.

5 Conclusions

(1) The thermal conductivity in the Datong Basin follows a pattern where igneous rocks exhibit the lowest values, metamorphic rocks have higher values than igneous rocks, and sedimentary rocks have a wider range of variations with higher over-
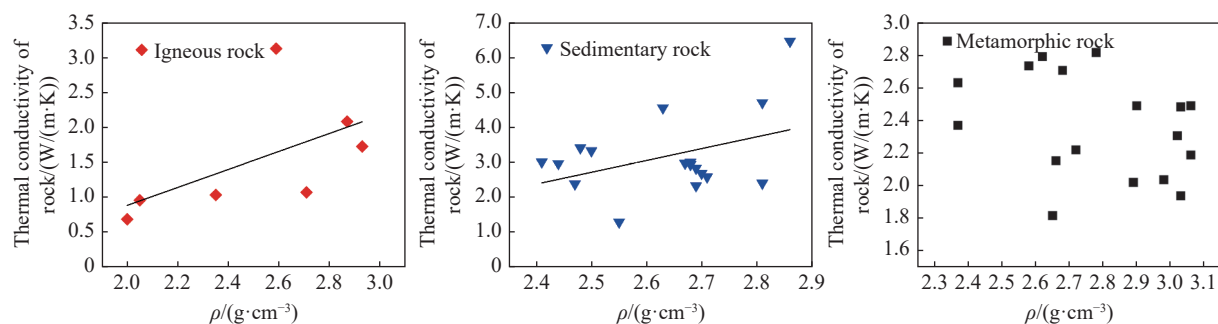
Fig. 11 Relation between thermal conductivity and density of rocks
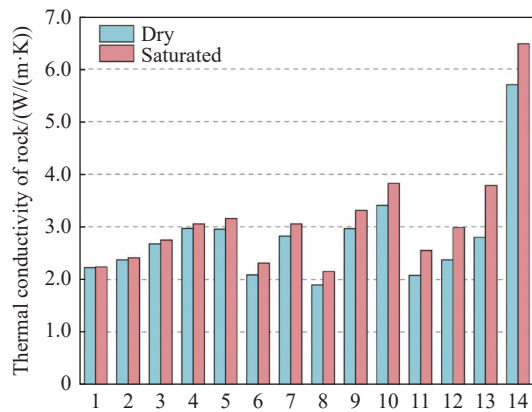
Fig. 12 Thermal conductivity of rocks under dry and water-saturated conditions

Notes: The serial number of horizontal coordinate is expressed respectively: 1-schist; 2-gneiss[①]; 3-limestone[①]; 4-limestone[②]; 5-sandstone[①]; 6-monzonitic granite; 7-dolomite[①]; 8-gneiss[②]; 9-mudstone; 10-sandstone[②]; 11-sandstone[③]; 12-sandstone[④]; 13-pebbly sandstone; 14-dolomite[②] (The upper corner marks represent different rock samples of the same lithology)

all values. The trend of rock thermal diffusivity aligns closely with thermal conductivity, demonstrating a clear positive correlation between the two, expressed by the equation $K = 2.733\kappa - 0.415$. The specific heat capacity shows a concentrated distribution among different lithologies, indicating similar heat storage capacities.

(2) The primary factor influencing the thermal conductivity of rocks in the Datong Basin is temperature. As temperature increases, the thermal conductivity of each lithology experiences varying degrees of reduction. Temperature correction equations for the corresponding lithologies have been derived for the Datong Basin. Through temperature correction, the in situ thermal conductivity of the Archaean gneiss thermal reservoir is calculated to be 1.907 W/(m·K).

(3) Rock density is not a direct determinant of thermal conductivity. Only homologous minerals with similar crystal structures exhibit a clear correlation, where higher density corresponds to greater thermal conductivity. In the study area, the thermal conductivity values of Archaean gneiss and Ordovician limestone thermal storage change minimally after water saturation. Due to challenges in controlling a single variable with stratigraphic factors, the relationship between stratigraphy and thermal conductivity is not universally applicable.

Acknowledgements

References

Cen M. 2015. Cenozoic tectonic evolution of Datong basin, northeastern margin of Ordos block. M. S. thesis. Hefei: Hefei University of Technology. (in Chinese)

Cui JW, Hou LH, Zhu RK, et al. 2019. Thermal conductivity properties of rocks in the Chang 7 shale strata in the Ordos Basin and its implications for shale oil in situ development. Petroleum Geology & Experiment, 41(02): 280−288. (in Chinese) DOI：10.11781/sysydz201902280.

Feng JK, Yao HJ, Chen L, et al. 2022. Ongoing lithospheric alteration of the North China Craton revealed by surface-wave tomography and geodetic observations. Geophysical Research Letters, 49: e2022GL099403. DOI：10.1029/2022GL099403.

Gao P. 2015. Analysis of rock thermal physical parameters and research on multi-field thermal effect coupled model. Ph. D. thesis. Jilin: Jilin University. (in Chinese)

Gao T. 2023. Present temperature field characteristics and influencing factors in Xiongxian geothermal field. M. S. thesis. Xian: Yangtze University. (in Chinese) DOI：10.26981/d.cnki.gjhsc.2023.001208.

Han Y, Bai XF, Zhang X. 2018. Discussion on geothermal resources and their exploitation and utilization mode in Shanxi Province. Geological Survey of China, 5(5): 13−20. (in Chinese) DOI：10.19388/j.zgdzdc.2018.05.02.

Hans-Dieter V, Rudiger S. 2003. Influence of temperature on thermal conductivity, thermal capacity and thermal diffusivity for different types of rock. Physics and Chemistry of the Earth, 28(9-11): 499−509. DOI：10.1016/S1474-7065(03)00069-X.

Jesse D, Merriman. 2023. A mineralogical model for thermal transport properties of rocks: Verification for low-porosity, crystalline

rocks at ambient conditions. Journal of Petrology, 64: 1−30. DOI：10.1093/petrology/egad012.

Lei XD, Hu SB, Li J, et al. 2018. Thermal properties analysis of bedrock in Beijing. Progress in Geophysics, 33(05): 1814−1823. (in Chinese) DOI：10.6038/pg2018BB0373.

Li JS. 2009. Reservoir rock thermal physical property test. Journal of Daqing Petroleum Institute, 33(05): 23−26. (in Chinese) DOI：10.3969/j.issn.2095-4107.2009.05.006.

Li X, Zhu CQ, Qiu NS, et al. 2023. Thermal conductivity of rocks and its influencing factors in northern Songliao Basin. Acta Geoscientica Sinica, 44(01): 70−83. (in Chinese) DOI：10.3975/cagsb.2022.092901.

Liu AR, Xu YJ, Liu CL, et al. 2021. Geological characteristics and tectonic evolution of Datong Basin. Geoscience, 35(05): 1296−1310. (in Chinese) DOI：10.19657/j.geoscience.1000-8527.2020.067.

Liu F, Zhang W, Wang GL, et al. 2023. Geothermal anomalies in the Xianshuihe area: Implications for tunnel construction along the Sichuan-Tibet Railway, China. Journal of Groundwater Science and Engineering, 11(3): 237−248. DOI：10.26599/JGSE.2023.9280020.

Ma F, Wang GL, Sun ZX, et al. 2019. An analysis of thermal conductivity in Songliao basin based on logging parameters. Acta Geoscientica Sinica, 40(02): 350−360. (in Chinese) DOI：10.3975/cagsb.2019.021101.

Meng J, Li N, Dong P, et al. 2022. Effects of phonon scattering channel on abnormal thermal conductivity of CaO and CaS. Journal of Shenyang University of Technology, 44(05): 525−529. (in Chinese) DOI：10.7688/j.issn.1000-1646.2022.05.08.

Miao SQ, Li HP, Chen G, et al. 2013. Progress of high temperature and high pressure experimental study on the thermal conductivity of the minerals and rocks. Progress in Geophysics, 28(05): 2453−2466. (in Chinese) DOI：10.6038/pg20130524.

Pan LY, Meng LJ, Sun FL, et al. 2022. Geothermal geological characteristics and resource potential in the north of Datong Basin, Shanxi Province. Geology in China, 50 (6): 1632. (in Chinese) DOI：10.12029/gc20220304001.

Qi K. 2021. Meso-Cenozoic lithospheric thermal-rheological structure and deep magmatic-thermal process in the WNCC. Ph. D. thesis. Xiaan: Northwest University. (in Chinese) DOI：10.27405/d.cnki.gxbdu.2021.002195.

Qiu NS. 2002. Characteristics of thermal conductivity and heat generation of rocks in basins in northwest China. Chinese Journal of Geology, (02): 196−206. (in Chinese)

Seipold U, Huenges E. 1998. Thermal properties of gneisses and amphibolites—high pressure and high temperature investigations of ktb-rock samples. Tectonophysics, 291(1-4): 173−178. DOI：10.1016/S0040-1951(98)00038-9.

Seipold U. 1998. Temperature dependence of thermal transport properties of crystalline rocks a general law. Tectonophysics, 291(1-4): 161−171. DOI：10.1016/S0040-1951(98)00037-7.

Shi QL. 2019. Tectonic thermal evolution characteristics of the Datong Basin. M. S. thesis. Beijing: China University of Geosciences. (in Chinese) DOI：10.27493/d.cnki.gzdzy.2019.000376.

Song JJ, Wang GL, Xing LX, et al. 2023. Influencing factors of rock thermal conductivity and applicability evaluation of its mixing law predictive models. Geothermics, 110: 102680. DOI：10.1016/j.geothermics.2023.102680.

Song XQ, Jiang M, Peng Q, et al. 2019. Characteristics and influencing factors of thermal property parameters of main rock strata in Guizhou Province. Acta Geologica Sinica, 93(08): 2092−2103. (in Chinese) DOI：10.19762/j.cnki.dizhixuebao.2019116.

Su H. 2021. Thermal geochemical characteristics of typical geothermal fields in Jizhong Depression. M. S. thesis. Nanchang: East China University of Technology. (in Chinese) DOI：10.27145/d.cnki.ghddc.2021.000170.

Sun SH, Liu SS, Wang J. 1996. Geothermal field and source rock evolution characteristics in Ordos Basin. Geotectonics and Metallogeny, (03): 255−261. (in Chinese) DOI：10.16539/j.ddgzyckx.1996.03.008.

Sun ZX, Zhang W, Hu BQ, et al. 2006. Features of heat flow and the geothermal field of the Qinshui Basin. Chinese Journal of Geophsics (S1): 93−98. (in Chinese) DOI：10.3321/j.

issn:0023-074X.2005.z1.016.

Tan FK. 2004. Contribution of lattice vibration to heat conduction. Journal of Minzu Normal University of Xingyi, (03): 71−73. (in Chinese) DOI：10.3969/j.issn.1009-0673. 2004.03.024.

Tavman IH. 1996. Effective thermal conductivity of granular porous materials. International Communications in Heat and Mass Transfer, 23(2): 169−176. DOI：10.1016/0735-1933 (96)00003-6.

Wang L, Ren Y, Deng F, et al. 2023. Study on calculation method of heat exchange capacity and thermal properties of buried pipes in the fractured rock mass-taking a project in carbonate rock area as an example. Energies, 16: 774. DOI：10.3390/en16020774.

Wang XJ. 2014. A brief analysis of the main thermal control structure and occurrence rule of geothermal resources in Shanxi Province. Huabei Natural Resources, 02: 85−87. (in Chinese) DOI：10.3969/j.issn.1672-7487. 2014.02.077.

Wei SC, Liu F, Zhang W, et al. 2022. Research on the characteristics and influencing factors of terrestrial heat flow in Guizhou Province. Journal of Groundwater Science and Engineering, 10(2): 166−183. DOI：10.19637/j. cnki.2305-7068.2022.02.006.

Wu FY，Lin JQ，Wilde SA, et al. 2005. Nature and significance of the Early Cretaceous giant igneous event in eastern China. Earth and Planetary Science Letters, 233(1): 103−119. DOI：10.1016/j.epsl.2005.02.019.

Xiong J, Lin HY, Ding HS, et al. 2020. Investigation on thermal property parameters characteristics of rocks and its influence factors. Natural Gas Industry, 7(3): 298−308. DOI：10.1016/j.ngib.2020.04.001.

Xu YL. 2015. The study on the formation and evolution of Datong Cenozoie Down-Faulted Basin. M. S. thesis. Taiyuan: Taiyuan University of Technology. (in Chinese) DOI：10. 7666/d.Y2798208.

Yang SZ, Zhang WR, Shen XJ. 1986. Saturated water test study on thermal conductivity of porous rocks. Acta Petrologica Sinica, (04): 83−91. (in Chinese) DOI：10.1007/ BF02658170.

Yu WQ. 2021. Deep process of thinning and destruction of heterogeneity in the North China Craton: Constraints from P-wave tomography. Institute of Geology, China Earthquake Administration. DOI：10.27489/ d.cnki.gzdds.2021.000025.

Zhang HY. 2016. Distribution and characteristics of geothermal resources in sedimentary basins in Shanxi Province. Huabei Natural Resources, (06): 115−116. (in Chinese) DOI：10.3969/j.issn.1672-7487.2016.06.040.

Zhang YL. 2019. Analysis of geothermal geological conditions in the area of Liudongying of Huairen sag in Datong Basin. Ground Water, 41(05): 15−17. (in Chinese) DOI：10.3969/j. issn.1004-1184.2019.05.006.

Zhao YX, Yang SZ, Zhang WR, et al. 1995. Temperature pressure experiment and analysis of rock thermal conductivity. Progress in Geophysics, 01: 104−113. (in Chinese)

Zhong YT, Kusky T, Wang L, et al. 2021. Alpine-style nappes thrust over ancient North China continental margin demonstrate large Archean horizontal plate motions. Nature Communications. DOI：10.1038/s41467-021-26474-7.

Zhou WL. 2021. Electrical structure of geothermal area in northeast of Datong Basin. Ph. D. thesis. Wuhan: China University of Geosciences. (in Chinese) DOI：10.27492/d.cnki. gzdzu.2021.000010.

Zhu CQ, Chen C, Yang YB, et al. 2022. Experimental study into the factors influencing rock thermal conductivity and their significance to geothermal resource assessment. Petroleum Science Bulletin, 7(03): 321−333. (in Chinese) DOI：10.3969/j.issn.2096-1693. 2022.03.029.

Zhu RX. 2018. Conclusion summary of the major research project "Destruction of North China Craton". Science Foundation of China, 32(3): 282−290. (in Chinese) DOI：10.16262/j.cnki. 1000-8217.2018.03.008.